International TOVS Study Conference-XIII Proceedings

VIIRS Sensor Performance

Carl Schueler , J. Ed Clement, Russ Ravella, Jeffery J. Puschell
Raytheon Santa Barbara Remote Sensing, Goleta CA 93117

Lane Darnton
Northrop Grumman Space Technologies, Redondo Beach CA 90278

Frank DeLuccia
The Aerospace Corporation, Los Angeles, CA 90245

Captain Tanya Scalione USAF and Hal Bloom
NPOESS Integrated Program Office, Silver Spring, MD 20910

Hilmer Swenson
The Aerospace Corporation, Silver Spring, MD 20910

***Abstract*-This paper summarizes the anticipated performance of the National Polar-orbiting Operational Environmental Satellite System (NPOESS) Visible Infrared Imaging Radiometer Suite (VIIRS) sensor. Predictions are generated from models and demonstration hardware based on the design described in a companion paper [1]. VIIRS risk-reduction will continue as the Engineering Development Unit (EDU) is assembled and tested over the next year facilitating performance verification and lowering flight unit development risk.**

I. INTRODUCTION

The Visible Infrared Imaging Radiometer Suite (VIIRS) sensor has been designed to provide the performance necessary to meet the Environmental Data Record (EDR) requirements defined by the National Polar-orbiting Environmental Satellite System (NPOESS) Integrated Program Office (IPO) in the NPOESS Integrated Operational Requirements Document-II (IORD-II) and the VIIRS Sensor Requirements Document (SRD) [2,3]. VIIRS successfully completed its Critical Design Review (CDR) in Spring 2002. Previous reports document the design prior to CDR [4-7], at CDR, and a companion paper documents refinements since CDR [7]. The next stage of development is completion of an Engineering Development Unit (EDU) in 2004. This EDU will allow verification of VIIRS Sensor performance prior to completion in 2005 of the first flight model which is scheduled for launch in 2006 on the NPOESS Preparatory Project (NPP) spacecraft.

Fig. 1 presents a mechanical view of the VIIRS design; a functional block diagram is provided in Fig. 2. At the preliminary design review (PDR), sensor performance was predicted using models developed by Raytheon SBRS. These models were the basis of the performance predictions previously reported for the initial sensor design. System-level simulations allowed Raytheon to conduct the sensor design and algorithm trades necessary to select the best balance of sensor performance, cost, design, and risk vs. system-level EDR performance.

In September 2002, the Raytheon VIIRS contract was transferred to TRW, now Northrup-Grumman Space Technologies (NGST), following TRW's receipt of an IPO contract to manage NPOESS and build the spacecraft. During the associated contract negotiation, responsibility for VIIRS EDR performance was transferred to NGST, limiting Raytheon SBRS' responsibility to production of VIIRS sensors in accordance with the sensor specification.

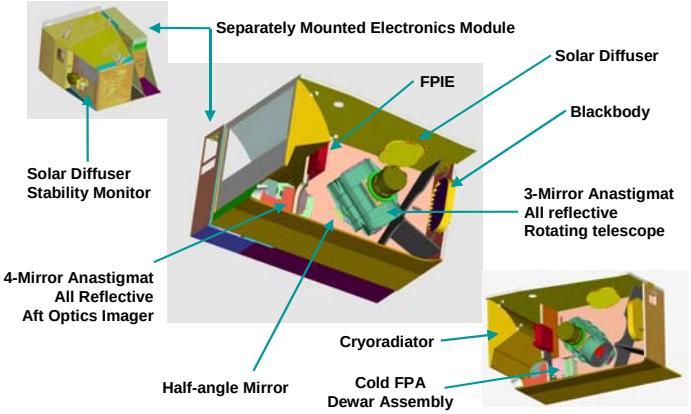

Figure 1. Single sensor design contains substantial flight hardware heritage.

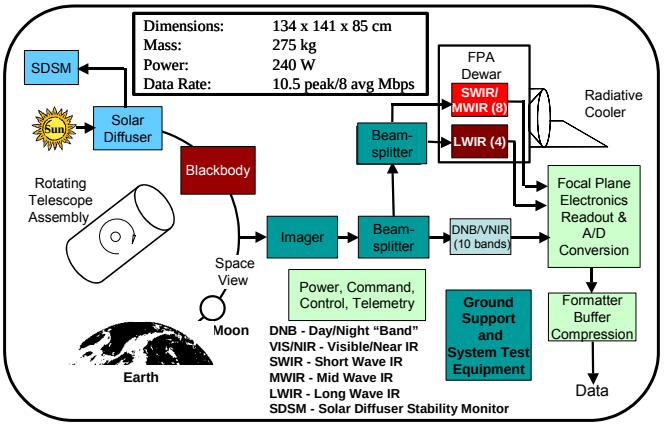

Figure 2: VIIRS block diagram traces photons from the Earth scene or internal calibration mechanisms to the focal plane arrays (FPA) and data output.

This paper presents sensor performance predictions for the updated design. These predictions are not only based on math models and simulations, but also take into account performance measured on recently completed engineering development hardware. These measurement results have both verified the accuracy of the models initially used to predict performance of these sensor subsystems and also increased confidence in updated predictions of sensor-level performance.

II. VIIRS PERFORMANCE MODELING

VIIRS sensor performance is predicted using models referenced in Fig. 3 and Table I. Some are VIIRS-specific, such as the Microsoft Excel SNR and dynamic-range model and the reflective and emissive band absolute radiometric error Mathcad models. Inputs to these models are derived from other modeling and simulation programs such as the optical transmission, modulation transfer function (MTF), forward and reverse ray tracing, and polarization models in Code V, ASAP, Excel, and the Sinda thermal model.

III. VIIRS PERFORMANCE

SNR, spectral radiance dynamic range, spatial MTF, polarization, radiometric accuracy, and structural and thermal performance under operational environments represent the primary sensor performance parameters that determine VIIRS overall EDR performance success.

Table II lists predicted horizontal sample intervals (HSI), MTF at the Nyquist frequency (0.5 HSI^{-1} cycles/km), and radiance dynamic range and SNR in each VIIRS spectral band. Specified and predicted SNR margins are shown on the far right. Note HSI is not the same as horizontal spatial resolution (HSR), although for most spectral bands the two are very close in value. HSR is defined as half the inverse of the spatial frequency at which the MTF equals 0.5.

The imagery EDR's fine HSR requirements were met with balanced optical and focal plane MTFs. The detector field stops in the moderate resolution (radiometry) bands were sized to provide improved HSI for coarser horizontal cell size (HCS) non-imagery EDRs, which also improves detector yield and lowers detector noise. VIIRS offers HSI <1.3 km nearly to edge-of-scan (EOS) in all bands, though required only to 43.6 degrees off-nadir. VIIRS offers finer nadir HSI than the Polar-orbiting Operational Environmental Satellite (POES) Advanced Very High Resolution Radiometer (AVHRR) and Terra/Aqua satellites MODerate resolution Imaging Spectroradiometer (MODIS), and with better nadir SNR via 3:1 aggregation following a patented design approach [9]. At EOS, the HSI is 4:1 finer in the cross-track dimension compared to AVHRR and MODIS, yet with comparable SNR, better than the Defense Meteorological Satellite Program (DMSP) Operational Line Scanner (OLS). Diverse Civil and DoD requirements therefore support one another through an integrated single-sensor design that balances improved imagery and spectro-radiometry.

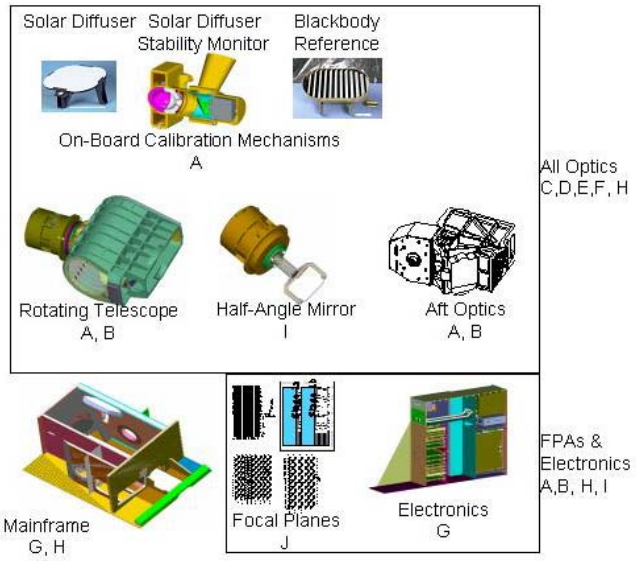

Figure 3: Simulations permit end-to-end sensor performance predictions.

Table I. Models used to predict VIIRS sensor performance.

Fig. 3 legend	Model Description
A	Signal to Noise Ratio (SNR)
B	Modulation Transfer Function (MTF)
C	Polarization Performance
D	Sequential Ray Trace
E	Non-sequential Ray Trace
F	Thin Films Design and Performance
G	Structural Design and Performance
H	Thermal Design and Performance
I	Electronics Simulation
J	Focal Plane Array (FPA) Performance

Table II shows two radiance ranges in "dual-gain" bands. In seven bands the saturation radiance and SNR requirements at low radiance made it impractical to meet both the dynamic range and sensitivity requirements with a single detector-channel gain setting. In these cases, Raytheon could have designed two separate detector arrays to meet the EDRs, one with high gain and excellent low radiance sensitivity, and another with lower gain and high saturation radiance. MODIS uses this approach for several spectral bands because when MODIS was designed in 1990, similar conflicting dynamic range and sensitivity requirements could not be met with one detector array. Raytheon since developed a readout integrated circuit (ROIC) capacitive transimpedance amplifier (CTIA) unit-cell with automatic gain control to cover the dynamic range, called "dual-gain." This allows the data necessary for the wide range of VIIRS EDRs to be accommodated with fewer detector arrays, reducing cost, data rate, and electronics mass, power, and volume.

The predicted SNR for all bands nadir to EOS for both single and dual-gain bands have margin of better than 97%. The Day/Night Band (DNB) CCD array provides a minimum SNR greater than 6 at EOS under its minimum radiance condition.

Table II. VIIRS Requirements and Predicted Performance by Spectral Band

		Band No.	Wave-length (μm)	Horiz Sample Interval (km Downtrack x Crosstrack)		Driving EDRs	Radi-ance Range	Ltyp or Ttyp	Signal to Noise Ratio (dimensionless) or NEΔT (Kelvins)		
				Nadir	End of Scan				Required	Predicted	Margin
VIS/NIR FPA	Silicon PIN Diodes	M1	0.412	0.742 x 0.259	1.60 x 1.58	Ocean Color	Low	44.9	352	483	37%
						Aerosols	High	155	316	827	162%
		M2	0.445	0.742 x 0.259	1.60 x 1.58	Ocean Color	Low	40	380	501	32%
						Aerosols	High	146	409	774	89%
		M3	0.488	0.742 x 0.259	1.60 x 1.58	Ocean Color	Low	32	416	573	38%
						Aerosols	High	123	414	747	80%
		M4	0.555	0.742 x 0.259	1.60 x 1.58	Ocean Color	Low	21	362	482	33%
						Aerosols	High	90	315	586	86%
		I1	0.640	0.371 x 0.387	0.80 x 0.789	Imagery	Single	22	119	135	13%
		M5	0.672	0.742 x 0.259	1.60 x 1.58	Ocean Color	Low	10	242	306	26%
						Aerosols	High	68	360	450	25%
		M6	0.746	0.742 x 0.776	1.60 x 1.58	Atmospheric Corr'n	Single	9.6	199	279	40%
		I2	0.865	0.371 x 0.387	0.80 x 0.789	NDVI	Single	25	150	212	41%
		M7	0.865	0.742 x 0.259	1.60 x 1.58	Ocean Color	Low	6.4	215	467	117%
						Aerosols	High	33.4	340	467	37%
CCD		DNB	0.7	0.742 x 0.742	0.742 x 0.742	Imagery	Var.	6.70E-05	6	6.2	3%
S/MWIR	PV HgCdTe (HCT)	M8	1.24	0.742 x 0.776	1.60 x 1.58	Cloud Particle Size	Single	5.4	74	109	47%
		M9	1.378	0.742 x 0.776	1.60 x 1.58	Cirrus/Cloud Cover	Single	6	83	156	88%
		I3	1.61	0.371 x 0.387	0.80 x 0.789	Binary Snow Map	Single	7.3	6.0	71	1084%
		M10	1.61	0.742 x 0.776	1.60 x 1.58	Snow Fraction	Single	7.3	342	461	35%
		M11	2.25	0.742 x 0.776	1.60 x 1.58	Clouds	Single	0.12	10	14	44%
		I4	3.74	0.371 x 0.387	0.80 x 0.789	Imagery Clouds	Single	270 K	2.500	0.236	68%
		M12	3.70	0.742 x 0.776	1.60 x 1.58	SST	Single	270 K	0.396	1.039	141%
		M13	4.05	0.742 x 0.259	1.60 x 1.58	SST	Low	300 K	0.107	0.051	111%
						Fires	High	380 K	0.423	0.353	20%
LWIR	PV HCT	M14	8.55	0.742 x 0.776	1.60 x 1.58	Cloud Top Properties	Single	270 K	0.091	0.057	60%
		M15	10.763	0.742 x 0.776	1.60 x 1.58	SST	Single	300 K	0.070	0.034	105%
		I5	11.450	0.371 x 0.387	0.80 x 0.789	Cloud Imagery	Single	210 K	1.500	1.004	49%
		M16	12.013	0.742 x 0.776	1.60 x 1.58	SST	Single	300 K	0.072	0.059	23%

The models used to predict SNR have been updated to take into account the most recent estimates of optical transmission based on recently completed tests of silver mirror witness samples, measured dichroic and spectral filter performance, and a reduction in optical aperture resulting in an f/6.2 system. Data from on-orbit MODIS and Enhanced Thematic Mapper (ETM) instruments has been used to more accurately predict end-of-life optical transmission that will result from degradation due to long term exposure to Earth-reflected ultraviolet radiation. Additionally, measured Noise Equivalent Irradiance (NEI) data from recently completed and in-process EDU focal planes indicates that the associated noise allocations in the SNR model will generally be achievable and with significant margin for many bands.

As discussed in the companion paper on VIIRS design changes since CDR[1], the sensor optical aperture stop has been repositioned from the primary mirror in the telescope (where it resides in MODIS) to a position immediately following the half angle mirror (HAM) derotator. Detailed optical analyses indicated that this was necessary to eliminate modulated instrument background (MIB) resulting from the VIIRS rotating telescope [1]. The emissive band radiometric error model was updated to include a more accurate representation of rotating optics emissions.

In parallel, the sensor thermal model was updated to provide higher fidelity predictions of internal sensor surface temperatures as a function of time in orbit (representative thermal data is shown in Fig. 4). These updated thermal predictions were used in the emissive band radiometric uncertainty model to verify that this modification to the optical design will achieve the excellent emissive band radiometric performance (Table III) predicted at CDR.

As part of this design update, a modest band-to-band registration improvement was possible. This was done by optimizing the location of the S/MWIR and LWIR detector field stops so that their locations better compensate residual pin cushion distortion in the overall sensor optical system. The updated band-to-band registration model predicts that the areas associated with spatially overlapping instantaneous fields of view (IFOVs) of specified moderate resolution S/MWIR and LWIR bands will be matched to better than 82%.

Table IV shows ASAP model predicted mirror coating and dichroic VNIR polarization. The 555 nm band is conservatively representative of 445-746 nm bands polarization, all specified at 2.5%.

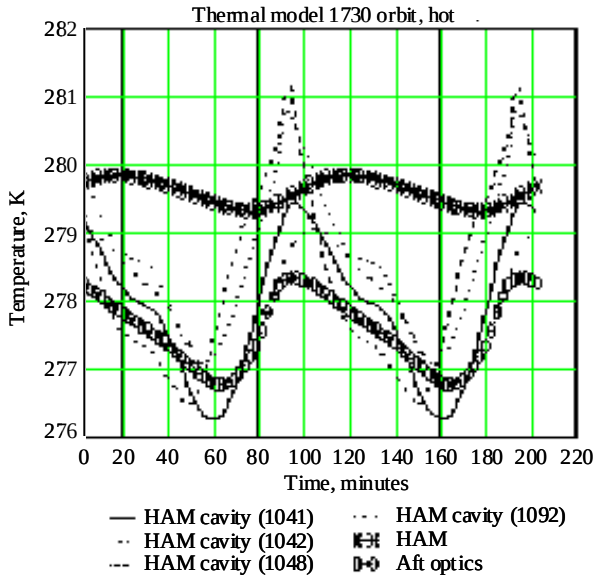

Figure 4. Updated VIIRS thermal modeling provides details of internal time-varying temperatures.

Table III. VIIRS provides excellent emissive band radiometric performance.

Parameter	VIIRS Center Wavelength (μm)				
	3.70	4.05	8.55	10.76	12.01
T typical (K)	270	300	270	300	300
Temp. Knowledge Effect (%)	0.32	0.24	0.14	0.09	0.08
Wavelength Knowledge Effect (%)	0.20	0.20	0.04	0.03	0.04
Integrated OOB Effect (%)	0.30	0.30	0.20	0.10	0.10
RVS Knowledge (%)	0.20	0.20	0.60	0.20	0.20
RVS Pedestal Knowledge	0.20	0.20	0.60	0.20	0.20
Emittance Knowledge (%)	0.20	0.20	0.20	0.20	0.20
Electronic Crosstalk (%)	0.20	0.20	0.20	0.20	0.20
Ghosting (%)	0.24	0.24	0.24	0.24	0.24
Polarization Knowledge Effect (%)	0.01	0.01	0.10	0.10	0.10
Earthshine Effect (%) (Tearth=343K)	0.029	0.025	0.009	0.008	0.007
AlSD Screen Emission (%) (Tinst=285K)	0.0293	0.0245	0.0091	0.0076	0.0071
SD Sunlight Scatter (%)	0.128	0.110	0.047	0.041	0.038
BB Skin Temp Effect (%) (Tinst=275K)	0.014	0.003	0.0	0.0	0.0
Surround Correction Effect (%) (Tinst=285K)	-0.031	-0.028	-0.013	-0.011	-0.01
Rad. Cal'n Model Stand. Dev. (%)	0.68	0.62	0.55	0.35	0.35
Allocation Reqmt (%)	0.7	0.7	0.6	0.4	0.4

Table IV. ASAP model predicts margin against polarization specification

Band name	Bandcenter (nm)	Specification (%)	-45 degrees	Zero degrees	+45 degrees
M1	412	3.0	1.30	2.00	2.90
M4	555	2.5	0.50	0.30	0.60
I2 & M7	865	3.0	0.70	0.04	0.02

IV. SUMMARY

The NPOESS VIIRS is a 22-band sensor employing a cross-track rotating telescope. The scene is imaged onto three focal planes separating VNIR, S/MWIR, and LWIR energy. The VNIR FPA has nine spectral bands, the S/MWIR FPA has eight spectral bands, and the LWIR FPA four spectral bands. The integral DNB capability provides a very large dynamic range low-light capability in all VIIRS orbits. VIIRS has been modeled via an extensive set of commercial ray tracing and structural and thermal design programs, as well as VIIRS specific radiometric models developed by Raytheon and validated against flight hardware measurements on earlier programs and on preliminary VIIRS engineering development hardware. The predicted performance based on these models shows margin against the sensor specification. The next major step in hardware performance assessment will be achieved with the completion and test of the VIIRS Engineering Development Unit (EDU) in 2004. EDU performance measurements will be used to verify the design, and to identify remaining design adjustments required to ensure that the flight models perform as required.

ACKNOWLEDGEMENTS

Phase I work was supported under NPOESS contract number F04701-97-C-0028 and partially by Raytheon funding, while post-PDR efforts are supported by NPOESS contract number F04701-01-C-0500. VIIRS sensor development is continuing under NGST contract 63549DGE2S to Raytheon SBRS. The authors wish to thank the excellent Raytheon, NGST, IPO and Aerospace Corporation design and review teams whose dedication and professionalism have made the results reported here possible.

REFERENCES

[1] T. Scalione, H. Swenson, F. De Luccia, N. Baker, C. Schueler, J. Clement, and L. Darnton, "Design Evolution of the NPOESS VIIRS Instrument Since CDR," International Geoscience and Remote Sensing Symposium (IGARSS) Proceedings, 25-30 July 2003.

[2] NPOESS IPO, Integrated Operational Requirements Document I (IORD II), version 6, 2002.

[3] NPOESS IPO, VIIRS Sensor Requirements Document, version 2b, 4 November 99.

[4] C. Welsch, H. Swenson, S. A. Cota, F. DeLuccia, J. M. Haas, C. Schueler, R. M. Durham, J. E. Clement, and P. E. Ardanuy, "VIIRS (Visible Infrared Imager Radiometer Suite): A Next-Generation Operational Environmental Sensor for NPOESS," International Geoscience and Remote Sensing Symposium (IGARSS) Proceedings, 8-14 July 2001.

[5] P. Ardanuy, C. Schueler, S. Miller, P. Kealy, S. Cota, J.M. Haas, and C. Welsch, "NPOESS VIIRS Design Process," SPIE 2001 4483-03

[6] C. Schueler, J. Clement, C. Welsch, F. DeLuccia, and H. Swenson, "NPOESS VIIRS Sensor Design Overview," SPIE 2001 4483-02

[7] C. Schueler, P. Ardanuy, P. Kealy, S.W. Miller, H. Swenson, J. M. Haas, F. DeLuccia, and S.Cota, "Remote Sensing System Optimization," IEEE Aerospace 2001

[8] C.Schueler and W.L. Barnes, "Next-Generation MODIS for Polar Operational Environmental Satellites," Journal of Atmospheric and Oceanic Technology, Vol. 15, No. 2, April 1998, pp. 430-439.

[9] R. Murphy, W. Barnes, A. Lyapustin, J. Privette, C. Welsch, F. DeLuccia, H. Swenson, C. Schueler, P. Ardanuy, and P. Kealy, "Using VIIRS to provide Data Continuity with MODIS," International Geoscience and Remote Sensing Symposium (IGARSS) Proceedings, 8-14 July 2001.

[10] C. Schueler, "Dual-use Sensor Design for Enhanced Spatioradiometric Performance," US patent 5,682,034; October 1997.

Proceedings of the Thirteenth International TOVS Study Conference

INTERNATIONAL ATOVS WORKING GROUP

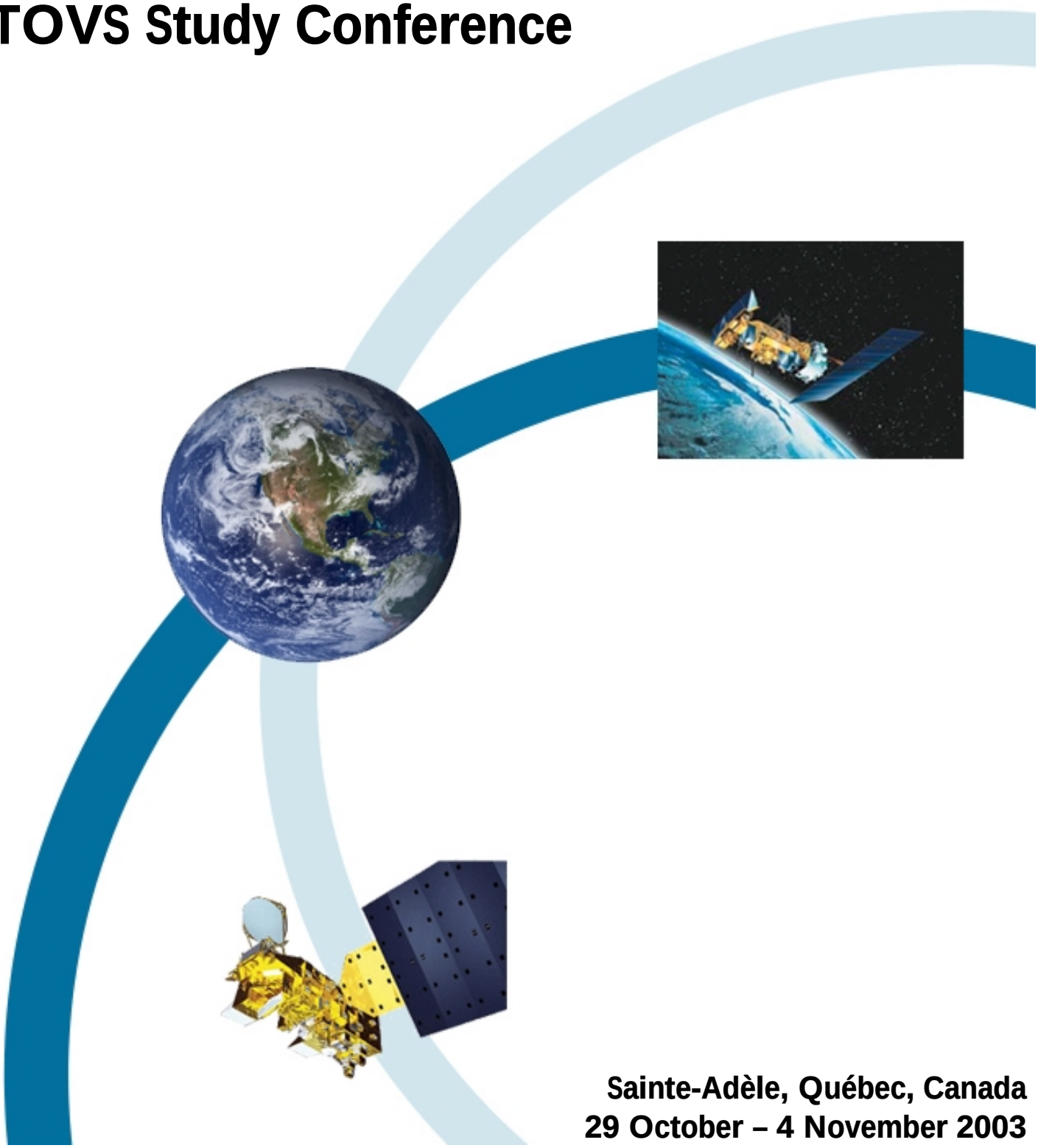

Sainte-Adèle, Québec, Canada
29 October – 4 November 2003